

peak of the ethylene molecule appear at the double- ζ level. However, their heights are much decreased when polarization functions are introduced. The deformation density of the formate, Fig. 2(c), agreed with that using the 4-31G and bond functions (Fuess *et al.*, 1982). A pair of the lone-pair peaks appear at the terminal O atoms in NO_2^- , NO_3^- and HCOO^- ions with angles of 100–110° to the bond axis, suggesting sp^2 hybridization of the O atoms as expected from the experimental deformation densities (Ohba *et al.*, 1985; and references cited therein). Although it is well known that unrealistic gross electron populations on atoms are often obtained by Mulliken population analysis when larger basis sets are used (Iwata, 1980), no drastic basis-set dependence in population analysis is seen from Table 2. The negative charge of NO_2^- , NO_3^- and HCOO^- is almost totally allocated to the O atoms.

The geometric distortion of NO_2^- is induced by an asymmetric $\text{Ag}^+ \cdots \text{O}$ short contact in the crystals of $\text{Ag}_2\text{Li}(\text{NO}_2)_3$. The N–O bond lengths and O–N–O bond angle are 1.24 (1), 1.29 (1) Å and 111.9 (8)° (Ohba, Matsumoto, Ishihara & Saito, 1986). In accord with the higher bond order of the shorter N–O bond axis, a bonding peak higher by 0.05 e Å⁻³ than that on the longer N–O bond axis was obtained on the MIDI4* deformation density. Another calculation was made to estimate the influence of the crystal field in $\text{LiNO}_2 \cdot \text{H}_2\text{O}$ on the charge density. The deformation density of the nitrite ion remained almost unchanged when the neighboring two Li^+ and two hydrate H atoms in hydrogen bonding were replaced by four point charges.

Note added in proof: An independent study of the role of polarization functions in the theoretical defor-

mation density of NO_2^- has recently been reported by Cruickshank & Eisenstein (1987). The results are similar to those given here.

References

- COPPENS, P. (1982). *Electron Distributions and the Chemical Bond*, edited by P. COPPENS & M. B. HALL, pp. 72–74. New York: Plenum.
- COPPENS, P. & LEHMANN, M. S. (1976). *Acta Cryst.* **B32**, 1777–1784.
- CRUIKSHANK, D. W. J. & EISENSTEIN, M. (1987). *J. Comput. Chem.* In the press.
- FEIL, D. (1985). Abstract of Sagamore VIII Conference, Review Lectures III.
- FIGGIS, B. N., REYNOLDS, P. A. & WRIGHT, S. (1983). *J. Am. Chem. Soc.* **105**, 434–440.
- FUESS, H., BATS, J. W., DANNÖHL, H., MEYER, H. & SCHWEIG, A. (1982). *Acta Cryst.* **B38**, 736–743.
- HERMANSSON, K., THOMAS, J. O. & OLOVSSON, I. (1980). *Acta Cryst.* **B36**, 1032–1040.
- IWATA, S. (1980). *Chem. Phys. Lett.* **69**, 305–312.
- KAMATA, S. & IWATA, S. (1987). To be published.
- KAY, M. I. & FRAZER, B. C. (1961). *Acta Cryst.* **14**, 56–57.
- KVICK, Å., LIMINGA, R. & ABRAHAMS, S. C. (1982). *J. Chem. Phys.* **76**, 5508–5514.
- LUNDGREN, J.-O., KVICK, Å., LIMINGA, R. & ABRAHAMS, S. C. (1985). *J. Chem. Phys.* **83**, 2426–2434.
- OHBA, S., KIKKAWA, T. & SAITO, Y. (1985). *Acta Cryst.* **C41**, 10–13.
- OHBA, S., KITaura, K., MOROKUMA, K. & SAITO, Y. (1979). *Annu. Rev. Inst. Mol. Sci. Okazaki*, pp. 21–22.
- OHBA, S., MATSUMOTO, F., ISHIHARA, M. & SAITO, Y. (1986). *Acta Cryst.* **C42**, 1–4.
- OHBA, S., TORIUMI, K., SATO, S. & SAITO, Y. (1978). *Acta Cryst.* **B34**, 3535–3542.
- PANT, A. K. & STEVENS, E. D. (1986). Private communication.
- RITCHIE, J. P. (1985). *J. Am. Chem. Soc.* **107**, 1829–1837.
- TATEWAKI, H. & HUZINAGA, S. (1980). *J. Comput. Chem.* **1**, 205–228.
- TELLGREN, R., RAMANUJAM, P. S. & LIMINGA, R. (1974). *Ferroelectrics*, **6**, 191–196.

Acta Cryst. (1987). **B43**, 85–92

A Deformation Electron Density Study of Potassium Oxalate Monohydrate at 100 K*

BY GLIGOR JOVANOVSki,† JOHN O. THOMAS AND IVAR OLOVSSON

Institute of Chemistry, University of Uppsala, Box 531, S-751 21 Uppsala, Sweden

(Received 28 October 1985; accepted 9 September 1986)

Abstract

The deformation electron density in $\text{K}_2\text{C}_2\text{O}_4 \cdot \text{H}_2\text{O}$ at 100 K has been studied using Hirshfeld-type deformation density functions [Hirshfeld (1971). *Acta Cryst.* **B27**, 769–781]. $\text{K}_2\text{C}_2\text{O}_4 \cdot \text{H}_2\text{O}$, $M_r = 184.24$, mono-

clinic, $C2/c$, $a = 9.0687$ (5), $b = 6.2128$ (3), $c = 10.5941$ (5) Å, $\beta = 110.820$ (1)°, $V = 557.92$ Å³, $Z = 4$, $D_x = 2.193$ Mg m⁻³, $\lambda(\text{Mo } K\alpha) = 0.71069$ Å, $\mu = 1.610$ mm⁻¹, $F(000) = 368$, $T = 100$ K. wR (F^2) values for 3543 $F_o^2 > 0$ reflections: 0.0568 (deformation refinement); 0.0623 (conventional refinement). The static deformation density for the H_2O molecule shows an O–H bond maximum of 0.25 e Å⁻³ and an oxygen lone-pair maximum of 0.35 e Å⁻³. The static

* Hydrogen Bond Studies. 152. Part 151: Gustafsson (1987).

† Permanent address: Institute of Chemistry, Cyril and Methodius University, Skopje, Yugoslavia.

peak maxima at the midpoints of the C–C and C=O bonds are $0.25\text{--}0.30 \text{ e } \text{Å}^{-3}$. $\Delta\rho$ maps exhibit clear π -bonding character in these bonds. The results from this work are compared with those from earlier room-temperature X-ray and neutron diffraction refinements [Hodgson & Ibers (1969). *Acta Cryst. B25*, 469–477; Sequeira, Srikanta & Chidambaram (1970). *Acta Cryst. B26*, 77–80].

Introduction

The present work forms part of a series of electron density studies of systems involving oxalate groups: $(\text{CH}_3)_2\text{NH}_2\text{HC}_2\text{O}_4$ (Thomas, 1977), $\text{NaHC}_2\text{O}_4 \cdot \text{H}_2\text{O}$ (Tellgren, Thomas & Olovsson, 1977; Delaplane, Tellgren & Olovsson, 1987). In combination with earlier extensive studies of $\alpha\text{-H}_2\text{C}_2\text{O}_4 \cdot 2\text{H}_2\text{O}$ (Stevens & Coppens, 1980; Stevens, 1980; Dam, Harkema & Feil, 1983; Coppens *et al.*, 1984; Wang, Tsai, Liu & Calvert, 1985), this makes it possible to compare the electron density features in $\text{C}_2\text{H}_2\text{O}_4$, C_2HO_4^- and $\text{C}_2\text{O}_4^{2-}$ groups. In this connection, it is important that the findings of the Coppens *et al.* (1984) study should be borne in mind; namely, that different accurate studies even of the same compound can give peaks of different heights and shapes.

The structure of potassium oxalate monohydrate, $\text{K}_2\text{C}_2\text{O}_4 \cdot \text{H}_2\text{O}$, has already been studied by various techniques: three-dimensional X-ray diffraction (Hendricks, 1935; Pedersen, 1964; Hodgson & Ibers, 1969); two- and three-dimensional neutron diffraction (Chidambaram, Sequeira & Sikka, 1964; Sequeira, Srikanta & Chidambaram, 1970); and also proton magnetic resonance (McGrath & Paine, 1964; Pedersen, 1966, 1968). The crystal structure consists of linear $-\text{H}_2\text{O}-\text{C}_2\text{O}_4^{2-}-\text{H}_2\text{O}-\text{C}_2\text{O}_4^{2-}-$ chains cross-linked by K^+ ions. The structure displays unusual coordination for a water molecule: the two neighbouring K^+ ions lie virtually in the H_2O plane.

Crystal data

The unit-cell parameters obtained in this work at 100 K (see below) are here compared with those derived by Hodgson & Ibers (1969) (hereafter HI) at room temperature.

	a (Å)	b (Å)	c (Å)	β (°)	V (Å ³)
Hodgson & Ibers (room temperature)	9.222 (3)	6.197 (2)	10.690 (5)	110.70 (3)	571.5
This work (100 K)	9.0687 (5)	6.2128 (3)	10.5941 (5)	110.820 (1)	557.92

Experimental

A single crystal of $\text{K}_2\text{C}_2\text{O}_4 \cdot \text{H}_2\text{O}$ (recrystallized from an aqueous solution) with dimensions $0.15 \times 0.17 \times 0.21$ mm was selected for data collection. Intensity data were collected on a Stoe-Philips four-circle

Table 1. *Some data on the refinements*

	Conventional refinement		Deformation refinement	
	$F_o^2 > 0$	$F_o^2 > 2\sigma(F_o^2)$	$F_o^2 > 0$	$F_o^2 > 2\sigma(F_o^2)$
Number of parameters refined		47		112
$wR(F^2)$	0.0623	0.0610	0.0568	0.0554
Conventional R	0.0351	0.0292	0.0333	0.0274
S	1.5414	1.6032	1.4186	1.4719
k (scale factor)	0.4891	0.4891	0.4923	0.4923
Number of reflections with $ dI/\sigma > 5$	35	19	35	19

diffractometer using graphite-monochromatized $\text{Mo K}\alpha$ radiation and an ω - 2θ step-scanning mode ($\Delta 2\theta = 0.04^\circ$; $6/3/1.5$ s per step after pre-scan). Fourteen reflections ($25 < 2\theta < 35^\circ$) were used for a least-squares refinement of cell parameters and orientation matrix. 3717 reflections of type $\pm h, k, \pm l$ (max. $h = 17$, max. $k = 12$, max. $l = 21$) were collected out to $\sin \theta/\lambda = 1.05 \text{ Å}^{-1}$. Of these, 166 had $F_o^2 < 0$; 567 had $F_o^2 < 2\sigma(F_o^2)$ and 697 had $F_o^2 < 3\sigma(F_o^2)$. Symmetry-related reflections were averaged; the $R_{\text{int}}(F^2)$ value for the averaging was 0.028. The total number of independent reflections thus obtained was 2455. The integrated intensities were corrected for Lorentz, polarization and absorption effects (transmission factors in range 73–80%). Three reference reflections monitored throughout the data collection showed intensity variations of less than 1%. The low temperature was obtained with an He gas Displex system. Maximum temperature fluctuation throughout the data collection was less than ± 5 K.

Two types of refinement were carried out: (a) conventional spherical-atom refinements; (b) deformation refinements. The starting values for the atomic coordinates and thermal parameters are taken from HI. All refinements were made with full-matrix least-squares techniques using the program *UPALS*. The spherical-atom scattering factors for K^+ , O, C and H and the anomalous-dispersion correction terms for K, O and C were taken from *International Tables for X-ray Crystallography* (1974). An isotropic type I extinction correction assuming a Lorentzian mosaic distribution was applied [$g = 670$ (130) and 900 (130) from the conventional and deformation refinements, respectively]; this implied a reduction of $\sim 12\%$ in the observed intensity of the most seriously extinguished reflection. The quantity refined was $\sum w(F_o^2 - \kappa F_c^2)$, where $w^{-1} = \sigma_o^2(F_o^2) + (kF_o^2)^2$. The constant k was fixed empirically at 0.02 on the basis of inspection of weighting analyses for different values of k .

All programs used for the various calculations made on the VAX 11/780 and Nord-100 computers have been described by Lundgren (1982).

Conventional spherical-atom refinements

In the last cycles of refinement, one scale factor, one isotropic extinction parameter, positional and

Table 2. Atomic positional parameters ($\times 10^5$), anisotropic thermal parameters ($\times 10^5 \text{ \AA}^2$) for non-hydrogen atoms and isotropic thermal parameter for H atom

The form of the anisotropic temperature factor is $\exp[-2\pi^2(U_{11}a^*h^2 + \dots + 2U_{12}(a^*b^*hk + \dots))]$.

First row: conventional refinement; second row: deformation refinement. The asphericity shift is the distance between the conventional and deformation refinement positions.

	x	y	z	Asphericity shift (Å)		
K	13430 (1)	83502 (2)	13355 (1)			
	13430 (2)	83500 (2)	13355 (2)	0.000 (1)		
O1	12187 (5)	26870 (7)	9103 (5)			
	12190 (7)	26877 (9)	9118 (6)	0.002 (1)		
O2	31836 (6)	48884 (7)	9225 (5)			
	31836 (7)	48885 (8)	9223 (5)	0.000 (1)		
OW	0	50570 (11)	0.25			
	0	50542 (20)	0.25	0.002 (1)		
C	23289 (6)	32557 (8)	5274 (6)			
	23303 (7)	32551 (10)	5267 (6)	0.002 (1)		
H	3529 (184)	41745 (217)	20077 (151)			
	3921	40675	19446*			
	U_{11}	U_{22}	U_{33}	U_{12}	U_{13}	U_{23}
K	252 (1)	453 (2)	147 (1)	-4 (1)	69 (1)	26 (1)
	248 (2)	448 (3)	143 (1)	1 (1)	67 (1)	28 (1)
O1	289 (4)	587 (8)	212 (4)	-53 (5)	162 (3)	-42 (4)
	286 (5)	575 (8)	209 (4)	-57 (5)	162 (3)	-50 (4)
O2	313 (5)	422 (7)	208 (4)	-90 (4)	111 (3)	-66 (4)
	314 (5)	419 (8)	205 (4)	-88 (5)	114 (3)	-71 (4)
OW	660 (9)	486 (11)	327 (6)	0	327 (6)	0
	648 (10)	481 (12)	327 (6)	0	325 (7)	0
C	222 (5)	398 (8)	121 (4)	11 (5)	66 (3)	-2 (4)
	219 (5)	381 (9)	122 (4)	-5 (5)	71 (3)	-15 (4)
H	$B_{\text{iso}} = 0.8 (3) \text{ \AA}^2$					
	$B_{\text{iso}} = 1.5 \text{ \AA}^2$ (fixed)					

* H position fixed (see text).

anisotropic thermal parameters for the non-H atoms and positional and isotropic thermal parameters for the H atom were refined. Further details are given in Table 1.

3543 reflections with $F_o^2 > 0$ were used in the last refinement. The final atomic positions and thermal parameters based on the refinement using all data with $F_o^2 > 0$ are listed in Table 2.*

Deformation refinements

Deformation density functions as proposed by Hirshfeld (1971) (see also Harel & Hirshfeld, 1975) were used. The charge density in the stationary molecule is expressed as a superposition of spherical free-atom densities, plus a deformation density

expressed as a linear combination of deformation functions localized on each atom (Harel & Hirshfeld, 1975), i.e.

$$\rho_c^{\text{stat}}(\mathbf{r}) = \sum_{\text{atom } i} \rho_{i,\text{sph}}^{\text{stat}}(\mathbf{r}) + \sum_{\text{atom } i} \sum_{\text{deformation function } j} c_{ij} \delta\rho_{ij}^{\text{stat}}(\mathbf{r}, \theta, \mathbf{n}, \mathbf{k})$$

where the c_{ij} 's are refinable deformation coefficients. The deformation functions $\delta\rho_{ij}^{\text{stat}}(\mathbf{r}, \theta, \mathbf{n}, \mathbf{k})$ have the general form: $Nnr^n e^{-\alpha r} \cos^n \theta_k$, where Nn is a normalization factor, n an integer between 0 and 4, r is the distance from the atom centre, θ_k is the angle between r and the k th of the chosen sets of polar axes, and α is a parameter that governs the radial breadth of the deformation functions on each type of atom. The c_{ij} 's were refined together with the positional and thermal parameters for the non-H atoms. The H-atom position was fixed by lengthening the OW-H distance obtained from the conventional refinement to 1.0 Å; an isotropic thermal parameter for H was fixed to 1.5 Å². Deformation coefficients up to $n \leq 3$ were refined for K⁺, O1, O2, OW and C, and for H up to $n \leq 1$. The α exponents used for K⁺, O, C and H were set to 6.0, 6.0, 5.5 and 4.0 Å⁻¹, respectively. All start values for the deformation coefficients were zero. Symmetry constraints were introduced for functions centred on O1 (m), O2 (m), C (m), OW (2) and H (cylindrical). No extra symmetry was imposed on K⁺. The weights used were as in the conventional refinements. The atomic coordinates and thermal parameters from the final cycle of deformation refinement with all data with $F_o^2 > 0$ are also given in Table 2. The resulting interatomic distances and angles from both conventional and deformation refinements are given in Table 3 together with values from earlier studies.

Discussion

We can first note an interesting negative thermal expansion in the b direction between room temperature and 100 K (*cf. Crystal Data*). As in the case of α -oxalic acid dihydrate discussed by Wang, Tsai, Liu & Calvert (1985), this effect is clearly related to an extreme anisotropy in the mean molecular interactions in the structure: more specifically, we see from Fig. 1 that the major H-bond components (the most anharmonic interaction potentials) lie in the ac plane.

The positional and thermal parameters derived by conventional and deformation refinement are compared in Table 2. Remarkably, there are no significant differences between them, as also evidenced by the negligible asphericity shifts given in Table 2. It can be noted that the position of the H atom derived from a conventional X-ray refinement at 100 K (this work) is much closer to that obtained from the room-temperature neutron study (Sequeira, Srikanta &

* Lists of structure factors from both the spherical-atom and the deformation refinements have been deposited with the British Library Document Supply Centre as Supplementary Publication No. SUP 43311 (65 pp.). Copies may be obtained through The Executive Secretary, International Union of Crystallography, 5 Abbey Square, Chester CH1 2HU, England.

Table 3. *Interatomic distances (Å) and angles (°)*

	This work (100 K)		Hodgson & Ibers (room temperature)	Sequeira, Srikanta & Chidambaram (room temperature)
	Conventional refinement	Deformation refinement		
C-C	1.573 (1)	1.570 (1)	1.5740 (24)	1.5698 (17)
C-O1	1.262 (1)	1.264 (1)	1.2595 (16)	1.2559 (14)
C-O2	1.255 (1)	1.255 (1)	1.2473 (17)	1.2487 (15)
O W-H	0.891 (15)	1.0*	0.80 (3)	0.9628 (33)
O W...O1	2.748 (1)	2.745 (1)	2.7602 (17)	2.7536 (17)
O1-C-O2	126.00 (5)	125.84 (6)	126.27 (12)	125.89 (9)
C-C-O1	116.27 (6)	116.29 (7)	115.76 (14)	116.24 (10)
C-C-O2	117.72 (6)	117.86 (7)	117.96 (13)	117.86 (9)
H-O W-H	104.0 (18)	104.3 (17)*	106.9 (32)	107.62 (33)
O1...O W...O1	115.19 (3)	115.24 (5)		118.82 (9)
H-O W...O1	5.7 (9)	5.6 (9)*		6.74 (14)
O W-H...O1	171.6 (14)	172.2 (14)*	165.9 (29)	169.66 (22)

* H position not refined.

Chidambaram, 1970) (hereafter SSC) than from the room-temperature X-ray study (HI).

Interatomic distances and angles derived here are compared with the room-temperature X-ray and neutron values in Table 3. There are some significant differences between the 100 K and room-temperature results: most notably, the characteristic shortening of C-O bonds as a result of librational motion.

The structure

A stereoscopic picture of the structure of $K_2C_2O_4 \cdot H_2O$ at 100 K is presented in Fig. 1. The structure has been described by Chidambaram, Sequeira & Sikka (1964) and by HI. Seven O atoms belonging to four different oxalate ions (three O1 and four O2 atoms) and one water O atom surround K^+ , with K-O distances in the range 2.727–2.998 Å (mean: 2.867 Å). The next nearest water O neighbour is at 3.277 Å.

As in the room-temperature HI and SSC studies, the oxalate anion is slightly non-planar at 100 K. The two parallel O1-C-O2 planes are separated by

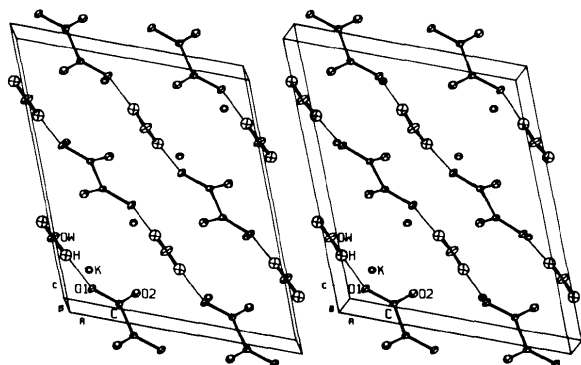
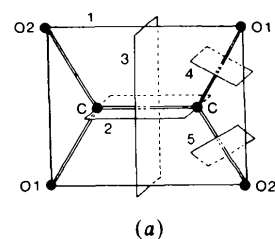
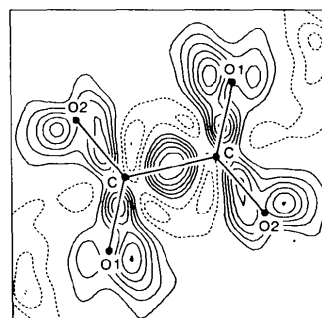


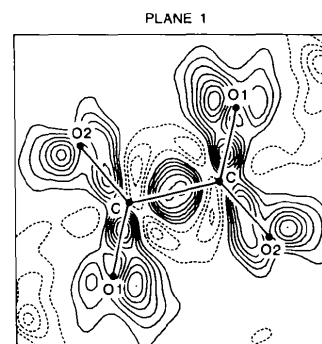
Fig. 1. A stereoscopic illustration of the structure. The thermal ellipsoids are drawn to include 50% probability. Covalent bonds are represented as thick and H...O1 bonds as thin lines.



(a)



(b)



(c)

Fig. 2. (a) The various planes in the C_2O_4 group for which the electron densities are plotted. (b) Dynamic and (c) static deformation density in the plane of the oxalate anion [plane 1 in (a)]. Contours are at $0.05 e \text{ \AA}^{-3}$ intervals. Negative contours are dashed and the zero contour is omitted.

0.021 (1) Å [at room temperature HI and SSC found 0.016 and 0.037 (6) Å, respectively].

The C–O1 bond length [1.262 (1) Å] (with O1 hydrogen bonded to the water O atom) follows the room-temperature tendency to be longer than the C–O2 bond in the same oxalate anion [1.255 (1) Å]. The difference at 100 K (0.007 Å) is smaller than the room-temperature X-ray value (0.012 Å) (HI) and the same as the neutron value (0.007 Å) (SSC). The O1–C–O2, C–C–O1 and C–C–O2 angles in $K_2C_2O_4 \cdot H_2O$ at 100 K are 126.00 (5), 116.27 (6) and 117.72 (6)°, respectively, demonstrating that the geometry of the oxalate ion is not significantly affected by cooling (except for the C–O distances). In general, the C–C bond of the α -oxalic acid molecule is not significantly longer than a normal single bond (1.54 Å), but is slightly lengthened as the acid molecule loses its protons (Küppers, 1973). The C–C bond length found in α - $H_2C_2O_4 \cdot 2H_2O$ by X-ray diffraction at 100 K (Stevens & Coppens, 1980; Wang, Tsai, Liu & Calvert, 1985) and neutron diffraction at 100 K (Feld & Lehmann, 1979) is 1.544 (1), 1.545 and 1.544 (1) Å, respectively. The C–C bond length in $(CH_3)_2NH_2HC_2O_4$ obtained from X-ray and neutron diffraction at room temperature (Thomas, 1977) is 1.545 (2) and 1.548 (2) Å; in $NaHC_2O_4 \cdot H_2O$, obtained by neutron diffraction at room temperature (Tellgren, Thomas & Olovsson, 1977) and at 120 K (Delaplane, Tellgren & Olovsson, 1984) it is 1.552 (1) and 1.553 (1) Å, respectively. In ammonium oxalate monohydrate studied by X-ray and neutron diffrac-

tion at room temperature (Taylor & Sabine, 1972), the fully ionized $C_2O_4^{2-}$ groups have C–C distances of 1.565 (14) and 1.557 (2) Å. In comparison with these values, the C–C bond is abnormally long in $K_2C_2O_4 \cdot H_2O$, 1.573 (1) Å (*cf.* Table 3). Two features are worth noting regarding the water molecule: the OW...O1 hydrogen-bond length is significantly shorter at 100 K than at room-temperature; also, the H–O–W angle [104.0 (18)°] is very close to the free-molecule value (104.5°).

The deformation electron density

Dynamic deformation densities are calculated as Fourier syntheses by setting the spherical atomic form factors (f_n 's) to zero, and using the refined Hirshfeld deformation coefficients (c_{ij} 's) and β_{ij} 's; the latter were also set to zero in the calculation of the static maps.

The reference state in all maps (Figs. 2–5) is a superposition of the free spherical electron densities for K^+ , O, C and H. As in earlier experimental results for α -oxalic acid dihydrate and for $NaHC_2O_4 \cdot H_2O$ (see *Introduction*), excess electron density is found along C–C, C–O1 and C–O2 as well as in the lone-pair regions of the O atoms (Figs. 2*b,c*). Although the C–C bond is abnormally long, the elliptical form of the electron density peak perpendicular to the C–C bond (Figs. 3*a-d*) indicates the existence of some π -bonding character (Coppens, 1984). As can be seen from Figs. 3(*e-h*), π -bonding character also

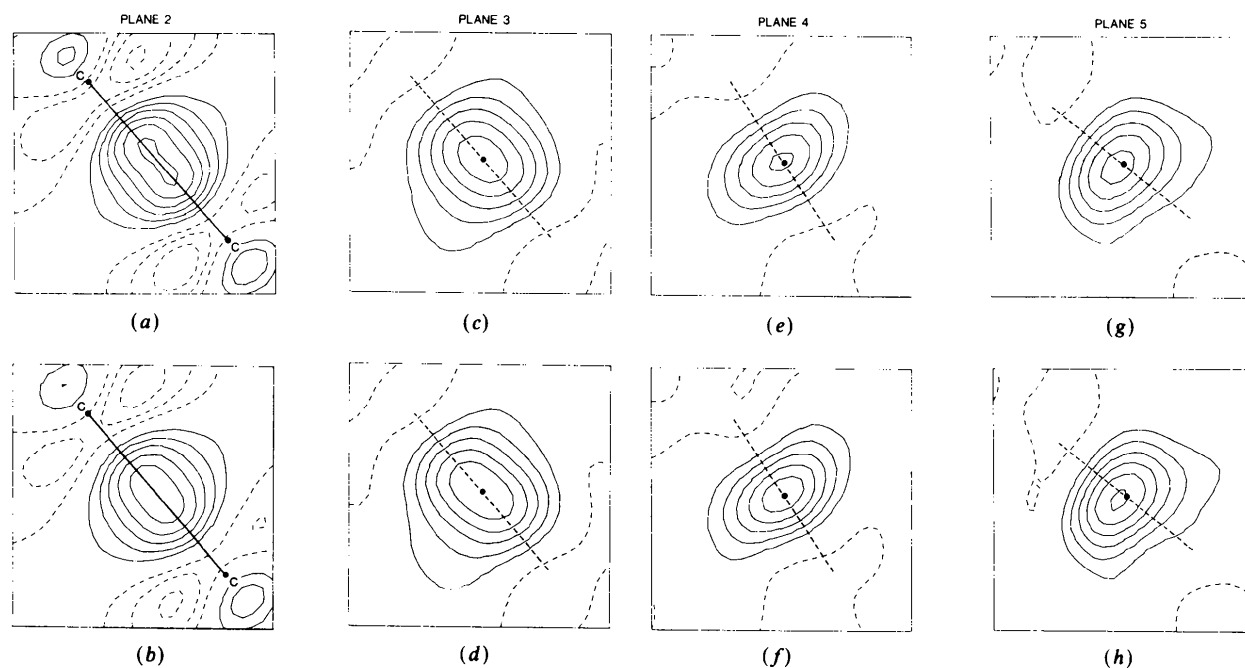


Fig. 3. Sections of the dynamic (upper row) and static (lower row) deformation densities of the oxalate anion in the planes 2, 3, 4 and 5 in Fig. 2(*a*). The C_2O_4 plane is indicated by dotted lines. Contours as in Figs. 2(*b*), (*c*).

Table 4. Bond and lone-pair (lp) peak heights ($e \text{ \AA}^{-3}$) for the deformation density in the plane of C_2O_4 and H_2O

Compound	Type of density	C-C	C-O1	C-O2	O1 (lp)	O2 (lp)	O3 (lp)	O4 (lp)	OW-H	OW (lp)	
$\alpha\text{-H}_2\text{C}_2\text{O}_4 \cdot 2\text{H}_2\text{O}$	Dynamic ^a	0.65	0.38	0.49	0.42	0.50 0.38					
	Static ^a	0.64	0.60	0.85	0.66	0.42 0.41					
	Dynamic ^b								0.36 0.42	0.45	
	Dynamic ^c	0.36	0.35	0.58	0.37	0.30 0.25			0.15 0.20	0.30	
$\text{NaHC}_2\text{O}_4 \cdot \text{H}_2\text{O}^d$	Dynamic	0.40	0.40*		0.15	0.20	0.15	0.10	0.15	0.15	
			0.20*		0.15		0.25	0.15	0.15		
$(\text{CH}_3)_2\text{NH}_2\text{HC}_2\text{O}_4^e$	Dynamic	0.40	0.40*		0.25	0.10	0.20	0.25			
			0.10*			0.20	0.30				
			0.40*								
			0.30*								
$\text{K}_2\text{C}_2\text{O}_4 \cdot \text{H}_2\text{O}^f$	Dynamic	0.25	0.30	0.25	0.30	0.30			0.15	0.25	
					0.15	0.25		0.20	0.25		
	Static	0.30	0.35	0.25	0.35	0.35			0.25	0.35	
					0.15	0.25		0.25	0.25		
$\text{LiHCOO} \cdot \text{H}_2\text{O}^g$	Dynamic								0.05	0.15	
									0.10	0.25	
$\text{LiNO}_2 \cdot \text{H}_2\text{O}$	Dynamic ^h								0.20	0.20	
									0.25	0.30	
	Static ^h									0.30	0.30
										0.35	0.28
Dynamic ⁱ									0	0	
									0	0	
$\text{LiNO}_3 \cdot 3\text{H}_2\text{O}^j$	Dynamic								0.25	0.15	
									0.30	0.30	
	Static									0.50	0.35
											0.45
$\text{LiOH} \cdot \text{H}_2\text{O}^k$	Dynamic								0.31	0.17	
									0.31		
									0.66	0.22	
	Static								0.66		

References: (a), (b), (c) 100 K deformation density from Stevens (1980), Stevens & Coppens (1980) and Wang, Tsai, Liu & Calvert (1985), respectively; (d) Room-temperature deformation density from Tellgren, Thomas & Olovsson (1977); (e) 298 K deformation density from Thomas (1977); (f) 100 K deformation density from this work; (g) Room-temperature deformation density from Thomas (1978); (h), (i) 295 K and 120 K deformation density from Hermansson & Thomas (1983) and Ohba, Kikkawa & Saito (1985), respectively; (j) 120 K deformation density from Hermansson, Thomas & Olovsson (1984); (k) 295 K deformation density from Hermansson & Thomas (1982).

* These values correspond to the deformation density along the four non-equivalent C-O bonds (C1-O1, C1-O2, C2-O3 and C2-O4) in the HC_2O_4^- ions in $\text{NaHC}_2\text{O}_4 \cdot \text{H}_2\text{O}$ and $(\text{CH}_3)_2\text{NH}_2\text{HC}_2\text{O}_4$.

appears in the C-O1 and C-O2 bonds. Similar results have been observed in $\text{NaHC}_2\text{O}_4 \cdot \text{H}_2\text{O}$ (Tellgren, Thomas & Olovsson, 1977) and α -oxalic acid dihydrate (Stevens & Coppens, 1980; Wang, Tsai, Liu & Calvert, 1985). Bond and lone-pair peak heights in the plane of C_2O_4 and H_2O are compared in Table 4.

Although the general characteristics of the deformation density maps for the $\text{C}_2\text{O}_4^{2-}$ ion are similar to those found in α -oxalic acid dihydrate and $\text{NaHC}_2\text{O}_4 \cdot \text{H}_2\text{O}$, there are some differences in peak heights and shapes. The electron density peak along the C-C bond in the $\text{C}_2\text{O}_4^{2-}$ plane (0.25 and 0.30 $e \text{ \AA}^{-3}$ in the dynamic and static maps) is almost spherical (cf. Figs. 2b,c), compared with the elongated peaks in α -oxalic acid dihydrate and $\text{NaHC}_2\text{O}_4 \cdot \text{H}_2\text{O}$. The density is also a little lower (cf. Table 4). As can be

seen from Table 4, the maximum peak heights in C-O1 and C-O2 (0.25-0.30 $e \text{ \AA}^{-3}$) are, on average, lower than or equal to the corresponding bonds in $\alpha\text{-H}_2\text{C}_2\text{O}_4 \cdot 2\text{H}_2\text{O}$ and $\text{NaHC}_2\text{O}_4 \cdot \text{H}_2\text{O}$. Similarly, the OW-H bond-density maxima (0.15 and 0.20 $e \text{ \AA}^{-3}$ for the dynamic and 0.25 $e \text{ \AA}^{-3}$ for the static density) and the maximum deformation density in the OW lone-pair region in the H_2O plane (0.25 and 0.35 $e \text{ \AA}^{-3}$ for the dynamic and static density, respectively) are in the same range as for corresponding bonds and lone-pair regions in many other hydrates (cf. Table 4 and Figs. 4a,b). The OW lone-pair region consists of a single symmetric peak (0.25 and 0.35 $e \text{ \AA}^{-3}$ in the dynamic and static map, respectively) very close to the OW nuclei (Figs. 4c-d). No tendency for double peaking is seen. As mentioned

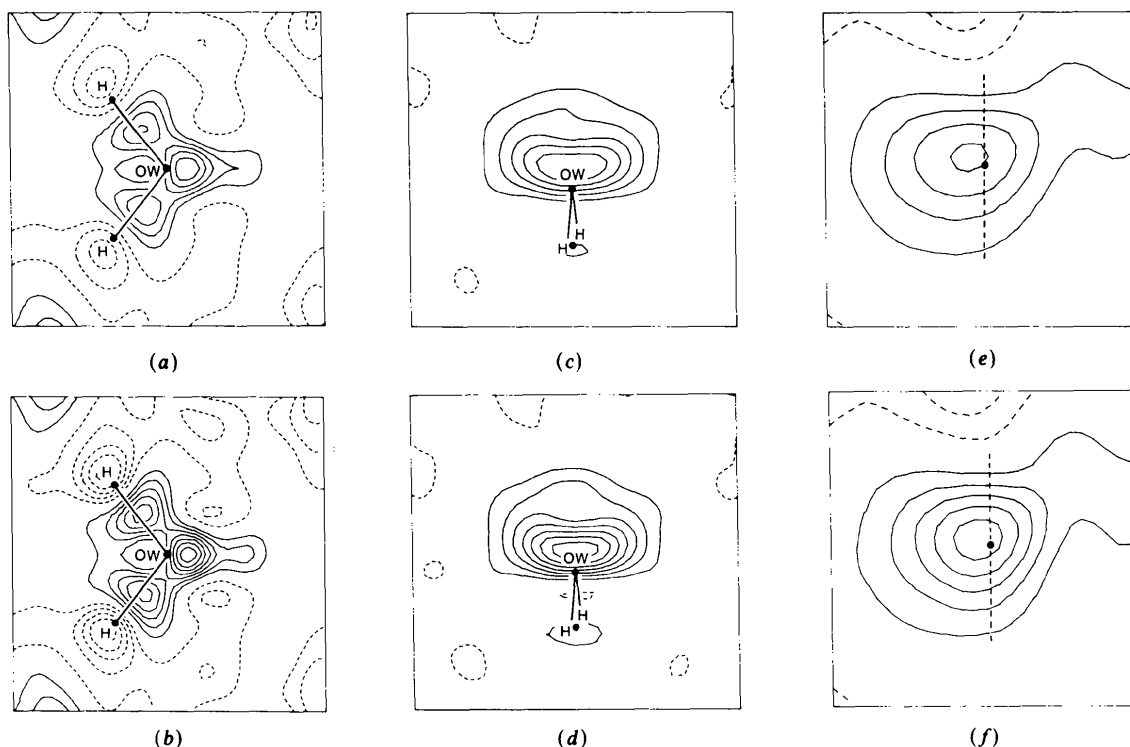


Fig. 4. Dynamic (upper row) and static (lower row) deformation density for the H_2O molecule. (a), (b) the molecular plane; (c), (d) the plane bisecting the $\text{H}-\text{O}-\text{H}$ angle; (e), (f) the plane perpendicular to the $\text{OW}-\text{H}$ bond at the bond midpoint. The H_2O plane is indicated by a dotted line. Contours as in Figs. 2(b), (c).

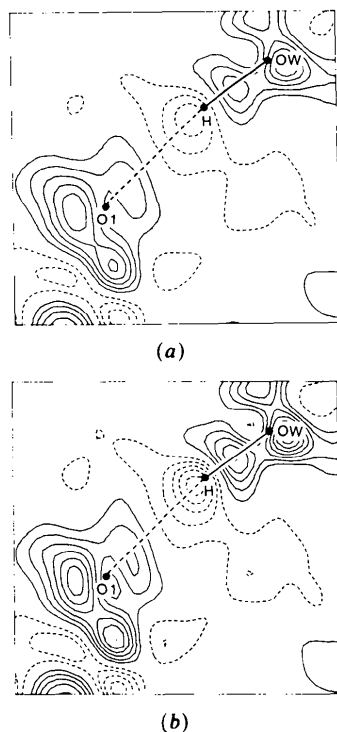


Fig. 5. Deformation density in the plane of the $\text{OW}-\text{H}\cdots\text{O1}$ hydrogen bond. (a) Dynamic map. (b) Static map. Sections as in Figs. 2(b), (c).

in the *Introduction*, the coordination of the water molecule is unusual: the two H atoms and two K^+ ions surrounding the OW atom are almost coplanar. The H-bond maps (Fig. 5) display features typical of intermediate hydrogen bonds: charge deficiency on the weakly bonded side of the H atom; charge excess in the O-H bond and in the lone-pair region of the hydrogen-bond acceptor. The general features of the deformation density in the $\text{OW}-\text{H}\cdots\text{O1}$ plane agree well with the observation made by Thomas (1977); namely, that the lone-pair deformation density in the direction of the hydrogen-bond acceptance is weaker (0.10 and $0.15 \text{ e } \text{\AA}^{-3}$ in dynamic and static maps) than in the non-bonding direction (0.25 and $0.30 \text{ e } \text{\AA}^{-3}$) (see also Figs. 2b,c). Similar experimental observations have been made for α -glycine (Almlöf, Kvik & Thomas, 1973), $\text{LiHCOO}\cdot\text{H}_2\text{O}$ (Thomas, 1978), $\text{NaHC}_2\text{O}_4\cdot\text{H}_2\text{O}$ (Delaplane, Tellgren & Olovsson, 1987), and also seen in theoretical calculations for $\text{NaHC}_2\text{O}_4\cdot\text{H}_2\text{O}$ (Lunell, 1984). As mentioned by Lunell (1984), this effect may be regarded as an artifact of the superposition of donor and acceptor deformation densities.

The experimental charges for K^+ , $\text{C}_2\text{O}_4^{2-}$ and H_2O deduced by summing the deformation coefficients for the even functions centred on each atom are $+0.71$, -1.38 and -0.04 e , respectively. The excessively high internal correlations between the deformation

coefficients make it difficult to estimate any error on these values.

This work has been funded by the Swedish Natural Science Research Council (NFR) and partly by the Macedonian Science Research Council. One of us (GJ) thanks the Cyril and Methodius University of Skopje for granting him leave of absence during his stay in Uppsala.

References

- ALMLÖF, J., KVICK, A. & THOMAS, J. O. (1973). *J. Chem. Phys.* **59**, 3901-3906.
- CHIDAMBARAM, R., SEQUEIRA, A. & SIKKA, S. K. (1964). *J. Chem. Phys.* **41**, 3616-3622.
- COPPENS, P. (1984). *J. Chem. Educ.* **61**, 761-765.
- COPPENS, P. *et al.* (1984). *Acta Cryst.* **A40**, 184-195.
- DAM, J., HARKEMA, S. & FEIL, D. (1983). *Acta Cryst.* **B39**, 760-768.
- DELAPLANE, R. G., TELLGREN, R. & OLOVSSON, I. (1984). *Acta Cryst.* **C40**, 1800-1803.
- DELAPLANE, R. G., TELLGREN, R. & OLOVSSON, I. (1987). In preparation.
- FELD, R. & LEHMANN, M. S. (1979). Unpublished results.
- GUSTAFSSON, T. (1987). *Acta Cryst.* **C43**. Submitted.
- HAREL, M. & HIRSHFELD, F. L. (1975). *Acta Cryst.* **B31**, 162-172.
- HENDRICKS, S. B. (1935). *Z. Kristallogr.* **91**, 48-64.
- HERMANSSON, K. & THOMAS, J. O. (1982). *Acta Cryst.* **B38**, 2555-2563.
- HERMANSSON, K. & THOMAS, J. O. (1983). *Acta Cryst.* **C39**, 930-936.
- HERMANSSON, K., THOMAS, J. O. & OLOVSSON, I. (1984). *Acta Cryst.* **C40**, 335-340.
- HIRSHFELD, F. L. (1971). *Acta Cryst.* **B27**, 769-781.
- HODGSON, D. J. & IBERS, J. A. (1969). *Acta Cryst.* **B25**, 469-477.
- International Tables for X-ray Crystallography* (1974). Vol. IV, pp. 99, 149. Birmingham: Kynoch Press. (Present distributor D. Reidel, Dordrecht.)
- KÜPPERS, H. (1973). *Acta Cryst.* **B29**, 318-327.
- LUNDGREN, J.-O. (1982). *Crystallographic Computer Programs*. Report UUIC-B13-4-05. Institute of Chemistry, Univ. of Uppsala.
- LUNELL, S. (1984). *J. Chem. Phys.* **80**, 6185-6193.
- MCGRATH, J. W. & PAINE, A. A. (1964). *J. Chem. Phys.* **41**, 3551-3555.
- OHBA, S., KIKKAWA, T. & SAITO, Y. (1985). *Acta Cryst.* **C41**, 10-13.
- PEDERSEN, B. (1966). *Acta Cryst.* **20**, 412-417.
- PEDERSEN, B. (1968). *Acta Chem. Scand.* **22**, 453-469.
- PEDERSEN, B. F. (1964). *Acta Chem. Scand.* **18**, 1635-1641.
- SEQUEIRA, A., SRIKANTA, S. & CHIDAMBARAM, R. (1970). *Acta Cryst.* **B26**, 77-80.
- STEVENS, E. D. (1980). *Acta Cryst.* **B36**, 1876-1886.
- STEVENS, E. D. & COPPENS, P. (1980). *Acta Cryst.* **B36**, 1864-1876.
- TAYLOR, J. C. & SABINE, T. M. (1972). *Acta Cryst.* **B28**, 3340-3351.
- TELLGREN, R., THOMAS, J. O. & OLOVSSON, I. (1977). *Acta Cryst.* **B33**, 3500-3504.
- THOMAS, J. O. (1977). *Acta Cryst.* **B33**, 2867-2876.
- THOMAS, J. O. (1978). *Acta Cryst.* **A34**, 819-823.
- WANG, Y., TSAI, C. J., LIU, W. L. & CALVERT, L. D. (1985). *Acta Cryst.* **B41**, 131-135.

Acta Cryst. (1987). **B43**, 92-96

Multidisciplinary Crystal Structure Analysis of a Bis(cadinane)

BY V. J. VAN GEERESTEIN AND J. A. KANTERS

Laboratorium voor Kristal- en Structuurchemie, Vakgroep Algemene Chemie, Rijksuniversiteit Utrecht, Transitorium III, Padualaan 8, 3205 TB Utrecht, The Netherlands

AND H. VAN KONINGSVELD

Afdeling der Technische Natuurkunde, Technische Hogeschool Delft, Lorentzweg 1, 2628 CJ Delft, The Netherlands

(Received 9 December 1985; accepted 25 August 1986)

Abstract

4,9-Diisopropyl-2,6a,12-trimethylperhydrobenzo-*[de]*naphthacene, $C_{30}H_{52}$, $M_r = 412.75$, orthorhombic, $P2_12_12_1$, $a = 10.106(1)$, $b = 17.831(3)$, $c = 29.666(5)$ Å, $V = 5346(1)$ Å³, $Z = 8$, $D_x = 1.026$ Mg m⁻³, $\lambda(\text{Mo } K\alpha) = 0.71069$ Å, $\mu(\text{Mo } K\alpha) = 0.05$ mm⁻¹, $F(000) = 1856$, room temperature, $R = 0.056$ for 2334 unique reflections. The crystal structure is pseudo $B22_12$ and the two independent molecules have identical conformations. The molecule consists of two cadinane units and represents a novel class of

saturated $C_{30}H_{52}$ pentacyclic isoprenoid hydrocarbons. The structure was solved by combining structural information obtained from NMR spectroscopy, mass spectrometry and Patterson synthesis, and then applying the *PATSEE* Patterson search procedure of E. Egert and G. M. Sheldrick using the devised models. NMR indicates 30 sp^3 C atoms, comprising two isopropyl and three methyl groups and a C_{21} pentacyclic skeleton. Mass spectrometry suggested that the molecule is composed of two sesquiterpane units and the Patterson function gives a pattern indicative of condensed cyclohexane rings. Molecular